

Document downloaded from:

<http://hdl.handle.net/10251/98648>

This paper must be cited as:

Ruiz Perez, G.; González-Sanchis, MDC.; Campo García, ADD.; Francés, F. (2016). Can a parsimonious model implemented with satellite data be used for modelling the vegetation dynamics and water cycle in water-controlled environments?. *Ecological Modelling*. 324:45-53. doi:10.1016/j.ecolmodel.2016.01.002



The final publication is available at

<http://doi.org/10.1016/j.ecolmodel.2016.01.002>

Copyright Elsevier

Additional Information

1 **Can a simple model implemented with satellite data be used for modelling**
2 **the vegetation dynamics and water cycle in water-controlled environments?**

3 Ruiz-Pérez, G. (*guruipr@cam.upv.es*)⁽¹⁾, González-Sanchis, M. (*macgonsa@gmail.com*)⁽²⁾, Del
4 Campo, A.D. (*ancamga@dihma.upv.es*)⁽²⁾, and Francés, F. (*f frances@hma.upv.es*)⁽¹⁾.

5 *(1): Research Group of Hydrological and Environmental Modelling (GIHMA), Research Institute of*
6 *Water and Environmental Engineering, Universitat Politècnica de València, Valencia, Spain*

7 *(2): Research Group in Forest Science and Technology (Re-ForeST), Research Institute of Water*
8 *and Environmental Engineering, Universitat Politècnica de València, Valencia, Spain*

9 **ABSTRACT**

10 Vegetation plays a key role in catchment's water balance, particularly in semi-arid
11 regions that are generally water-controlled ecosystems. Nowadays, many of the
12 available dynamic vegetation models are quite complex and they have high
13 parametrical requirements. However, in operational applications the available
14 information is quite limited. Therefore parsimonious models together with
15 available satellite information can be valuable tools to predict vegetation
16 dynamics. In this work, we focus on a parsimonious model aimed to simulate
17 vegetation and hydrological dynamics, using both field measurements and
18 satellite information to implement it. The results suggest that the model is able to
19 adequately reproduce the dynamics of vegetation as well as the soil moisture
20 variations. In other words, it has been shown that a parsimonious model with
21 simple equations can achieve good results in general terms and it is possible to
22 assimilate satellite and field observations for the model implementation.

23 **KEY WORDS:** satellite data; parsimonious; dynamic vegetation model; semi-arid;
24 water fluxes

25 **1. Introduction**

26 A better understanding of the components of catchments' water balance has
27 traditionally been one of the main objectives of the hydrological community
28 (Gerten *et al.*, 2004). To this end, it is certainly well-known that the vegetation
29 plays a key role in a catchment's water balance particularly in semi-arid regions
30 (Laio *et al.*, 2001). In these water-controlled ecosystems, the vegetation controls
31 the hydrological processes through its influence on interception, infiltration,
32 evapotranspiration, surface runoff and, consequently, groundwater recharge
33 (Rodriguez-Iturbe *et al.*, 2001). The vegetation key role on controlling the
34 hydrological cycle is such that the actual evapotranspiration may account for
35 more than 90% of the precipitation (Pilgrim *et al.*, 1988; Huxman *et al.*, 2005).
36 From here that reliable estimates of spatial and temporal variations of actual
37 evapotranspiration as well as precipitation are vital to obtain reliable estimates of
38 the available water resources (Andersen, 2008). In spite of this, traditionally, very
39 few hydrological models had incorporated the vegetation dynamic as a state
40 variable, neglecting in this way most of the interactions with vegetation and
41 vegetation dynamics themselves (Lee and Pielke, 1992; Parlange and Katul,
42 1992; Walker and Langridge, 1996; Alvenäs and Jansson, 1997; Snyder *et al.*,
43 2000; Aydin *et al.*, 2005). In fact, most of them are able to represent fairly well the
44 observed discharge at the catchment outlet, but usually including the vegetation
45 as a static parameter (Quevedo and Francés, 2008).

46 In the last decades, the number of hydrological models which explicitly take into
47 account the vegetation development as a state variable has increased
48 substantially and considerable efforts have been made to understand and
49 reproduce adequately the interactions between the vegetation and the water
50 cycle. However, most of the time, these models are difficult to constrain because
51 of the high number of parameters that are required to be estimated (Quevedo
52 and Francés, 2008). This represents a particularly challenging task, especially
53 considering that in operational applications the available information is frequently
54 quite limited, in particular for arid and semi-arid regions which often in some
55 respects could be categorized as ungauged basins (Andersen, 2008).

56 Therefore parsimonious models, together with available remote sensing
57 information, can be valuable tools to predict vegetation dynamics. For this
58 reason, we have focused on the use of the parsimonious and dynamic vegetation
59 LUE-model proposed by Pasquato *et al.* (2014). Briefly, the parsimonious LUE-
60 model simulates gross primary production (GPP) as a function of absorbed
61 photosynthetically active radiation (APAR) and the vegetation light use efficiency
62 (LUE). Net primary production (NPP) is then calculated taking into account
63 maintenance respiration. This model is focused particularly on simulating foliar
64 biomass, which is obtained from NPP through an allocation equation based on
65 the maximum LAI sustainable by the system (Pasquato *et al.*, 2014).

66 However, since LUE is a parsimonious and conceptual model, some vegetation
67 processes have been neglected. It is important to check that the most relevant
68 processes are being captured by the model. For this reason, the present study
69 compares the capability of this parsimonious model against a physically-based

70 model in reproducing the interaction between vegetation and water. The selected
71 physically-based model was the well-known Biome-BGC (Thornton *et al.*, 2002).
72 The models were applied in a semi-arid forest experimental plot (East of Spain)
73 and their performances were analyzed against field data (daily soil water content
74 and transpiration). The parsimonious LUE-Model was calibrated using remote
75 sensing data and validated using the field observations, while the BIOME-BGC
76 model was implemented only using the field measurements.

77 In this way, we want to know if the use of a parsimonious model together with
78 remote sensing data is an option comparable to the use of a physically-based
79 model together with field observations. This question is very interesting in those
80 cases in which there are not field measurements. Zhang *et al.* (2011) showed
81 how model's predictions can be improved using satellite imagery combined with
82 field data. However, there are still many open questions regarding the remote
83 sensing's applicability and robustness. Pasquato *et al.* (2014) highlighted the
84 importance to evaluate firstly the remote sensing data to be used in order to
85 ascertain the value of the information that can be extrapolated from them, taking
86 into account the fact that external conditions and the structure of vegetation
87 canopy can alter the computed vegetation indices values (Jackson and Huete,
88 1991).

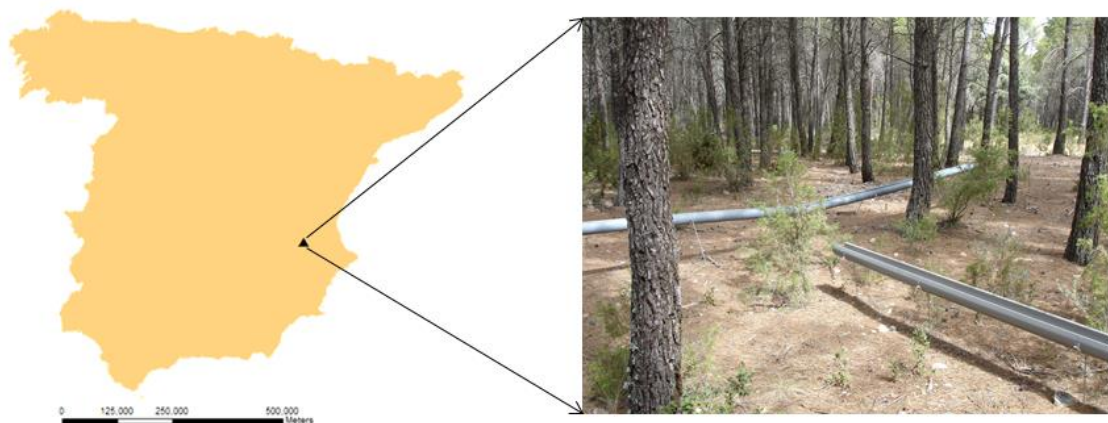
89 In most of the applications, satellite data is used combined with field data. But,
90 actually, it will be rare to have field measurements for model implementation in
91 practical applications. Therefore, in this paper we address the following two
92 questions: (1) is the proposed parsimonious model capable to satisfactory
93 simulate vegetation and hydrological dynamics or a more complex model is

94 needed? and, (2) can satellite products be used to implement a dynamic
95 vegetation model or are field measurements totally necessary?

96 **2. Study area**

97 The study site is an experimental plot located in the Public Forest *Monte de la*
98 *Hunde y Palomeras* in the East part of Spain (Figure 1). The sandy-silty loam
99 soils predominate with high concentration of carbonate (16-38%, pH 7.7-8.2). Soil
100 thickness ranges between 50 and 60 cm. The climate is Mediterranean with a
101 mean annual rainfall of 466 mm and a mean annual temperature of 13.7 °C
102 (1960-2007). The mean annual reference evapotranspiration is 749 mm. Using
103 the Köppen climate classification, the climate of this area is classified as semiarid
104 (González-Sanchis *et al.*, 2015).

105 The vegetation in the experimental plot is characterized by an homogeneous
106 Aleppo pine (*Pinus halepensis*) plantation of high tree density with scant
107 presence of other tree species either in forest gaps or as understory species
108 (e.g., *Quercus ilex* sbsp. *ballota*, *Pinus pinaster*) (Molina and del Campo, 2012).
109 This place has been previously studied and modeled. Information about the
110 results of the previous studies can be found at González-Sanchis *et al.* (2015),
111 Molina and del Campo (2012) and, del Campo *et al.* (2014).



112

113 Figure 1. Location of the experimental plot study site. Detailed view of the 60 years old aleppo pine
114 plantation, control plot, used for this work.

115 3. Field measurements

116 Measurements of Soil Water Content (SWC) and transpiration were carried out in
117 an experimental plot of 30x30 m (Del Campo *et al.*, 2014). Transpiration was
118 measured in 4 trees by considering the diametrical distribution (<20.5 cm low,
119 20.5-26.5 cm medium, >26.5 cm high). Four trees were selected: one of the high,
120 one of the low and two of the medium diameter class. Sap flow velocity was
121 measured through the HRM method (Burgess *et al.*, 2001; Hernandez-Santana
122 *et al.*, 2011; Williams *et al.*, 2004) in all sample trees and programmed to average
123 every hour. In each tree a HRM sap flow sensor (HRM sensor, ICT International,
124 Australia) was placed at 1.3 m height and at the north side.

125 SWC was measured using 9 FDR sensors (EC-TM, Decagon Devices Inc.,
126 Pullman, WA), placed at 30 cm depth and considering either tree influence or not
127 (i.e., under projected crown or not). SWC was continuously measured for the
128 whole period every 20 minutes. Field sensor calibrations were carried out by

129 determining the gravimetric water content in four sampling dates (saturation, field
130 capacity, between field capacity and wilting point and wilting point) to obtain the
131 full range of SWC in the study site (Del Campo *et al.*, 2014). In this way, plant
132 transpiration and soil moisture were obtained in the experimental plot during the
133 observational period from 27/03/2009 to 31/05/2011.

134 The Leaf Area Index (LAI) was estimated on field using a LAI-2000 sensor (LI-
135 COR, 1991) only once at the beginning of the work. Readings were taken under
136 direct solar radiation (Molina and Del Campo, 2011) with a 270° view cap and
137 with the sensor always shaded to avoid light dispersions affecting sensor
138 readings (LI-COR, 1991). The measured LAI has a value of 2.6.

139 At the end, we used the following field measurements to carry out the
140 implementation of the complex model: (1) daily transpiration data calculated as
141 an average which takes into account the number of trees included in each
142 diameter class (low, medium and high), and (2) daily SWC data calculated
143 according to the vegetation cover, assuming that the sensors under tree
144 influence (mean value) were representative of the area covered by vegetation
145 and the sensors without tree influence (mean value) were representative of bare
146 soil. The fraction covered by pine in the experimental plot is the 84% with a tree
147 density of 1489 tree/ha.

148 **4. Satellite data**

149 In this work, we analyzed the following satellite products provided by NASA
150 (NASA Land Processes Distributed Active Archive Center (LP DAAC)): the
151 Normalized Difference Vegetation Index (NDVI), included in the MOD13Q1 and

152 MYD13Q1 products; the Leaf Area Index (LAI), included in the MOD15A2; and
153 the MYD15A2 products and the actual evapotranspiration (ET), included in the
154 product MOD16A2. For the coverage of the study site, the h17v05 tile is required,
155 where h and v denote the horizontal and vertical tile number, respectively. The
156 MODIS vegetation index datasets provided in Hierarchical Data Format (HDF)
157 were imported to GeoTIFF format by MODIS Reprojection Tool (MRT) (software
158 provided by NASA) and reprojected from the Integerized Sinusoidal (ISIN)
159 projection to Universal Transform Mercator projection system.

160 The NDVI data is provided by NASA every 16 days and with a spatial resolution
161 of 250X250 m. On the other hand, the LAI data is provided every 8 days and with
162 a spatial resolution of 1X1 km. Both MODIS products were analyzed from
163 18/02/2000 to 02/02/2013. Finally, the ET datasets provided by NASA are
164 evaluated using Mu *et al.*'s algorithm (2011) based on Penman Monteith equation
165 (Monteith, 1965). This algorithm uses the following satellite information to be
166 implemented: land cover classification, albedo, LAI and fPAR (fraction of the
167 photosynthetically active radiation). It is available from 01/01/2000 to 26/12/2012,
168 provided every 8 days and with a spatial resolution of 1X1 km. As the study
169 experimental plot (described above) is only of 30X30 m and it is completely
170 covered by one satellite pixel, we used directly the value of NDVI, LAI and ET
171 from this pixel. In other words, interpolation techniques were not needed.

172 As a result of the dataset analysis, only NDVI was finally used to calibrate LUE
173 model. Despite the fact that all analyzed satellite products (NDVI, LAI and ET)
174 showed a marked seasonal quasi-sinusoidal behavior as expected (Figure 2), the
175 values of LAI were significantly lower than the one measured in the field. Satellite

176 LAI values ranged from 0.8 to 1.2, while the measured one was 2.6. This field
177 value is in agreement to values reported in literature (Sabaté *et al.*, 2002;
178 Sprintsin *et al.*, 2007; Vicente-Serrano *et al.*, 2010) for the same species and
179 under similar climatic conditions. Thus, the use of satellite LAI was finally
180 dismissed. Likewise, as the Mu's algorithm employed to calculate ET uses the
181 MODIS LAI, the use of satellite ET was also rejected. Hence, we used only the
182 NDVI data from 18/02/2000 to 02/02/2013 to carry out the calibration of the LUE
183 model. It should be underline that LAI and ET products are calculated by NASA
184 using models, and at least for this particular pixel, they did not work.

185 **5. Models**

186 **5.1. LUE-Model**

187 ***Hydrological sub-model***

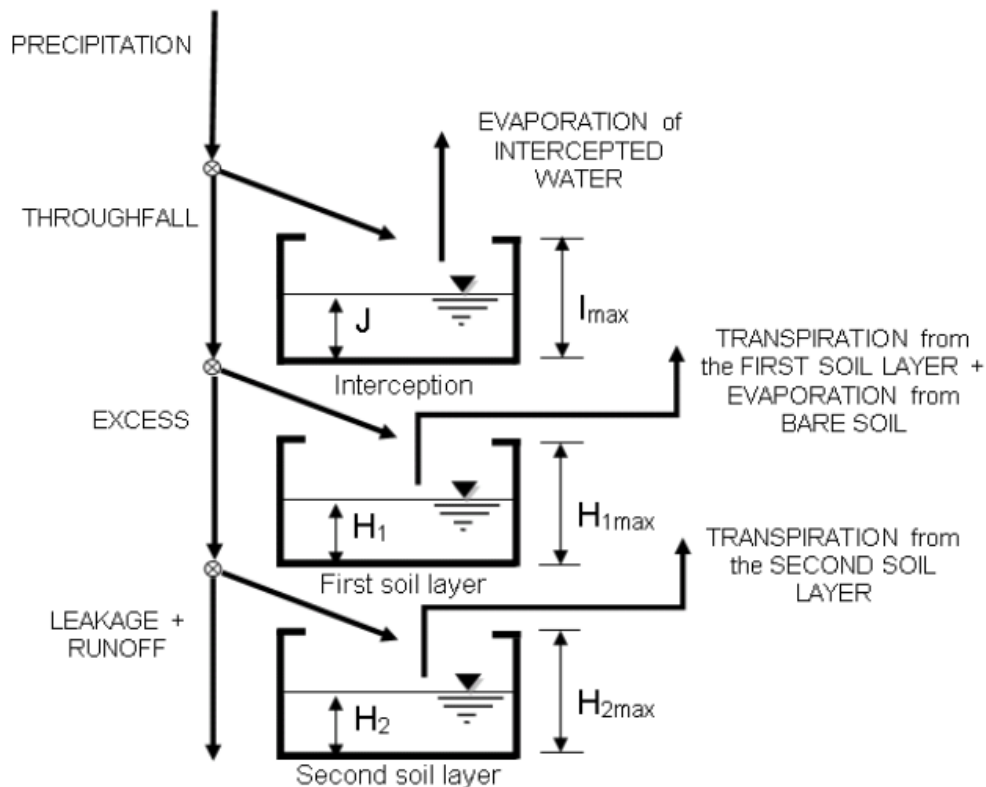
188 The dynamic vegetation model was coupled with a hydrological model based on
189 a tank-based schema (Figure 2). A more detailed description of the hydrological
190 model used can be found in Quevedo and Francés (2008), Pasquato (2013) and
191 Pasquato *et al.* (2014).

192 Briefly, the first tank represents the amount of water retained by the canopy. This
193 water can only exit from this tank by direct evaporation. On the other hand, the
194 soil depth is divided into two layers: a shallow layer that involves the processes of
195 bare soil evaporation and superficial roots transpiration, and a second underlying
196 layer that provides soil moisture to deeper roots (Figure 2).

197 Transpiration (both from the shallow layer and from the deeper layer) is
198 calculated according to FAO recommendations (Allen et al., 1998): the
199 transpiration is obtained using the reference evapotranspiration (ET_0) multiplied
200 by a water stress factor (ζ) and by a factor related to the current leaf area index
201 (LAI) simulated by the dynamic vegetation model, as shown in equation 1.
202 Through this factor, the state of vegetation affects the hydrological fluxes and,
203 consequently, the water storage in the different tanks.

$$T_i = (ET_0 - EI) * \min(1, LAI) * \zeta * Z_i \quad (1)$$

204 where T_i is the transpiration from the i soil layer, EI is the evaporation of the
205 intercepted water and Z_i is the percentage of roots in the i soil layer. The
206 expression $\min(1, LAI)$ is the factor which replaces the crop factor recommended
207 by the FAO 56.



208

209 Figure 2. Schema of the hydrological sub-model (Pasquato *et al.*, 2014)

210 ***Dynamic Vegetation sub-model***

211 Many approaches for estimating plant biomass production (Field *et al.*, 1995;
 212 Running *et al.*, 2004; Montaldo *et al.*, 2005; Pasquato *et al.*, 2014) are based on
 213 the use of the light use efficiency (LUE) concept. The LUE is the proportionality
 214 between plant biomass production by terrestrial vegetation and absorbed
 215 photosynthetically active radiation in optimal conditions. However, this efficiency
 216 can be affected by stress conditions. The key factors contributing to the variation
 217 of this efficiency are: soil moisture content, air temperature (Landsberg and
 218 Waring, 1997; Sims *et al.*, 2006), and nutrient levels (Gamon *et al.*, 1997;
 219 Ollinger *et al.*, 2008).

220 Our LUE model simulates the leaf biomass (BI, kg DM m⁻² ground) as follows
221 (Pasquato *et al.*, 2014:

$$\frac{dB_l}{dt} = (LUE * \varepsilon * PAR * fPAR - Re) * \phi_l - k_l * B_l \quad (2)$$

222 where ε takes into account the reduction in LUE due to stress sources. In this
223 study, as it was applied in a water-controlled catchment, the stress factors
224 considered were only the water stress and the temperature stress. The nutrient
225 levels were not considered, because they are not the dominant stress source in
226 this area. The water stress factor connects the dynamic vegetation model with
227 the hydrological model. Re is the respiration, ϕ_l is the fractional leaf allocation and
228 k_l is the leaf natural decay factor to reproduce the senescence. Finally, PAR and
229 fPAR are the photosynthetically active radiation and the fraction of PAR absorbed
230 by the canopy respectively. More information about these terms can be found in
231 Pasquato (2013).

232 The daily PAR was obtained from the incident global radiation provided by a
233 nearby meteorological station using a constant ratio of 0.48 MJ (PAR) MJ⁻¹
234 (global radiation) (McCree, 1972). The fPAR was obtained using the Beer-
235 Lambert law:

$$fPAR = 0.95 * (1 - e^{-k*LAI}) \quad (3)$$

236 where k is the light extinction coefficient and LAI is the leaf area index simulated
237 by the model. The LAI is simulated through the specific leaf area (SLA) and the
238 vegetation fractional cover (f_v):

$$LAI = B_l * SLA * f_v \quad (4)$$

239 However, Dawson *et al.* (1998) showed that NDVI is influenced by leaf water
240 content. For this reason, some authors (William and Albertson, 2005; Pasquato
241 *et al.*, 2014) recommend the use of a water stress factor to make comparable the
242 LAI with the NDVI as shown in equation 5.

$$LAI_r = LAI * \overline{\zeta_{10}} \quad (5)$$

243 where the LAI_r is the LAI comparable with NDVI and $\overline{\zeta_{10}}$ is the average plant
244 water stress of the previous 10 days as proposed by William and Albertson
245 (2005).

246 **5.2. Biome-BGC Model**

247 As representative of a complex model, this paper uses the Biome-BGC 4.2 model
248 (Thornton *et al.*, 2002) for two reasons. Firstly, the model is well documented,
249 both technically and in scientific publications; second, the source code of the
250 model is publicly available on the Internet (NTSG 2001). Furthermore, it is also
251 widely used as a benchmark during global change analysis (e.g., Schimel *et al.*
252 1994). Complete descriptions of the model have been carried out in many studies
253 (Pietsch *et al.*, 2003; Tatarinov and Cienciala, 2006; Chiesi *et al.*, 2007; Maselli *et*
254 *al.*, 2009).

255 Briefly, the model operates in a $1m^2$ scale, with a daily time step and describes
256 the dynamics of energy, water, carbon and nitrogen in a defined type of terrestrial
257 ecosystem (deciduous broadleaf forest, coniferous forest or grassland). The
258 model requires: daily climate data, information of the general environment (soil,
259 vegetation and site conditions) and 34 parameters describing the eco-

260 physiological characteristics of vegetation such as specific leaf area, water
261 interception coefficient or light extinction coefficient. BIOME-BGC is provided with
262 default ecophysiological parameters sets for the major biome types, but these
263 must be modified to adapt to Mediterranean ecosystems (Chiesi *et al.*, 2007).
264 Water cycle calculation includes daily canopy interception, evaporation,
265 transpiration, soil evaporation, soil water potential, soil water content and outflow.

266 **6. Methodology**

267 This paper implements the LUE-Model following two steps: (1) calibration of the
268 model using the satellite NDVI and (2) validation using the available field
269 measurements (transpiration and SWC). The performance of the model is then
270 compared to that of the BIOME-BGC model by comparing the simulation results
271 between them and to the field observations. Thus, the simulated period of both
272 models includes the period with available field data (27/03/2009 to 31/05/2011),
273 as well as two different precipitation scenarios: dry (year 2005) and wet (year
274 2010). In particular, we computed the amount of 'blue water' (water in liquid form
275 used for the human needs or which flows out the ecosystems) and the amount of
276 'green water' (water having the vapor for resulting from evaporation and
277 transpiration processes) in order to obtain and compare the blue/green rate (B/G)
278 using both modeling alternatives.

279 Due to observational and model conceptualization errors and time and space
280 scale effects, any mathematical model must use effective parameters for a better
281 reproduction of reality (Blöschl and Sivalapan, 1995; Francés *et al.*, 2007). The
282 main reason of the calibration of a mathematical model is therefore to obtain the
283 effective values of its parameters.

284 The hydrological sub-model has six parameters to be calibrated: (1) maximum
285 interception storage, (2) the wilting point soil moisture, (3) field capacity soil
286 moisture, (4) optimal point soil moisture, (5) effective depth soil of the first layer
287 and (6) effective depth soil of the second layer. With regards to the dynamic
288 vegetation sub-model, there are seven parameters to be calibrated: (1) LUE,
289 Light Use Efficiency, (2) coverage factor, (3) distribution of roots factor, (4)
290 maximum LAI sustainable by the system, (5) light extinction coefficient, (6) SLA,
291 Specific Leaf Area, and (7) optimal temperature.

292 To calibrate both sub-models (thirteen parameters) we used the available NDVI
293 data from 18/02/2000 to 02/02/2013. As NDVI is sensitive to green leaf biomass,
294 it can be primarily employed to monitor the photosynthetically active biomass of
295 plant canopies, and the relationships between NDVI and LAI have been strongly
296 demonstrated. For this reason, the selected objective function was the Pearson's
297 correlation coefficient between the simulated LAI_r and the satellite NDVI. Firstly,
298 calibration was carried out using a manual adjustment of parameter's values and
299 using values recommended in literature for each parameter (some sources were:
300 Ceballos and Ruiz de la Torre, 1979; Calatayud *et al.*, 2000 and others). Later, a
301 genetic algorithm called Evolver was used to optimize the calibration process.
302 Finally, the model was validated using daily field measurements of SWC and
303 transpiration.

304 The BIOME-BGC was calibrated and validated using daily field sap flow and soil
305 moisture data. For calibration, the 70% of the field data were used, while the
306 remaining 30% were used to validate the model. Since it is a model which works
307 at 1m² scale (individual scale), it was applied in various trees and, later, we

308 calculated an average of these 'individual' results. A more detailed description of
309 this process can be found in González-Sanchis *et al.* (2015).

310 The performance of both models was analyzed comparing the simulation results
311 to the field observations. The selected goodness-of-fit indexes were the Root
312 Mean Square Error (RMSE), the Nash and Sutcliffe efficiency index (E) and the
313 Pearson correlation coefficient (only for the LAI evaluation).

314 As the main objective of this paper is to know if a simple model implemented only
315 using satellite data can be used as alternative against a well-known physically-
316 based model implemented using field measurements, we ran both models for a
317 long period and, later, we compared the differences between them.

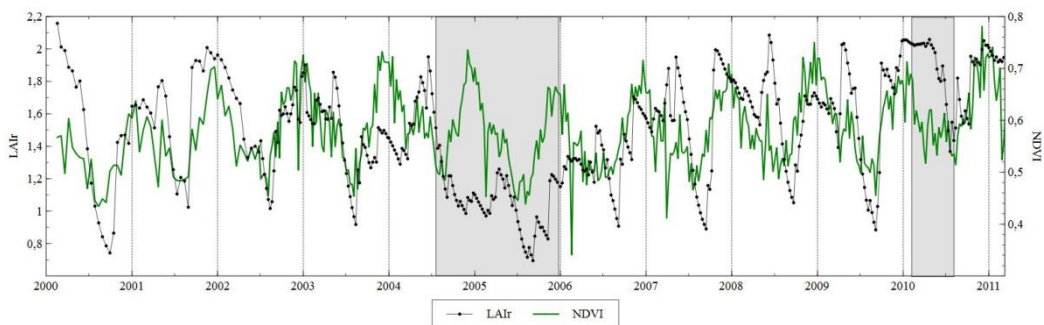
318 Finally, the B/G water ratio was calculated using the results from each model. In
319 our models, on one hand, the Blue water is the excess water from the upper soil:
320 i.e., surface runoff plus deep percolation. And, on the other hand, the Green
321 water is calculated as the sum of the amount of water transpired by plants, the
322 amount of water evaporated from the bare soil and the amount of water
323 evaporated from the interception.

324 **7. Results**

325 In general, the calibration of the LUE model showed a strong positive relationship
326 between the LAI_r and the NDVI provided by satellite in the entire period (see
327 Figure 3), with a Pearson correlation coefficient of 0.635.

328 However, during the calibration, despite the fact that generally the simulated
329 peak values of LAI_r coincided with those of NDVI, a significant disagreement

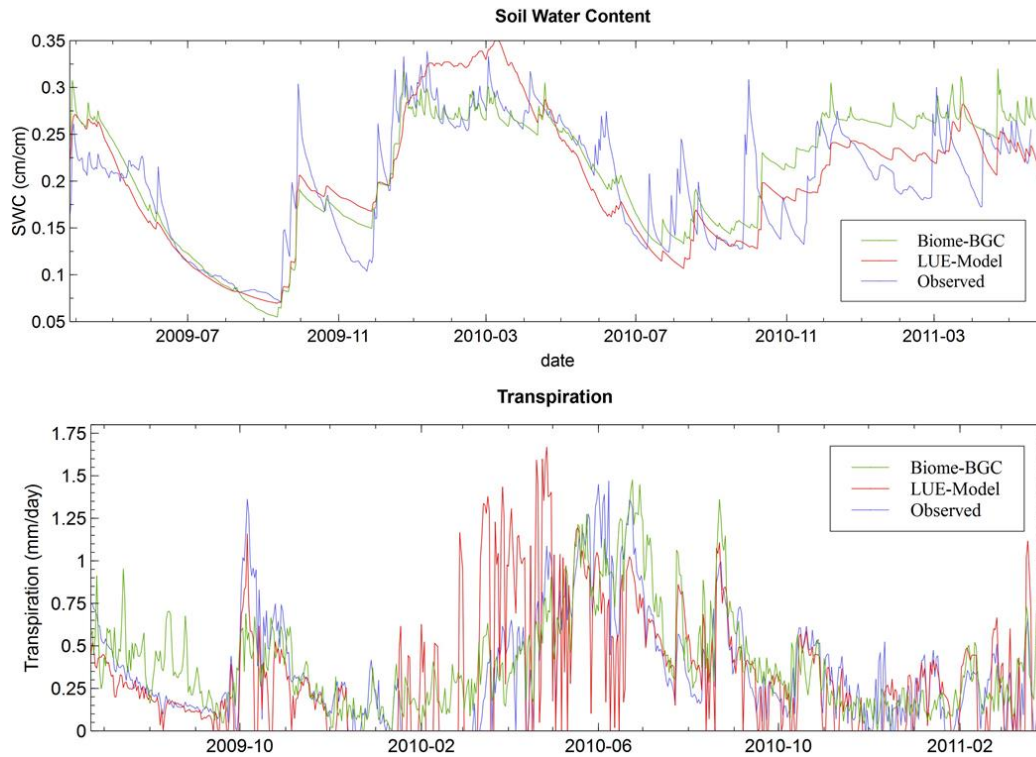
330 between both variables was obtained during two specific periods (shaded in
331 Figure 3). During the first period, from July 2004 to December 2005, the LAI_r and
332 the NDVI series were totally uncorrelated, especially during the beginning of this
333 period. Likewise, in the second period, spring 2010, the simulated LAI_r
334 maintained a high value while the NDVI decreased substantially.



335

336 Figure 3. Comparison between LAI_r simulated by the model and NDVI from satellite. The shaded
337 areas correspond to the two specific periods with a significant disagreement between simulated
338 LAI_r and satellite NDVI.

339 The validation of the LUE-Model with the field measurements showed a general
340 agreement between the simulated and the measured SWC and transpiration,
341 although the former appears to be more accurately reproduced (see Table II).
342 The major disagreement in the prediction of transpiration values occurred during
343 the spring of 2010, which is the same period where the simulated LAI_r and the
344 NDVI were noticeably uncorrelated.



345

346 Figure 4. Transpiration and SWC simulated by both models and measured in field

347 As mentioned before, the calibration and validation of the BIOME-BGC has been
 348 previously carried out in González-Sanchis *et al.* (2015) and the results are
 349 summarized in Table II. The model predicts accurately SWC and transpiration,
 350 although like the LUE model, the BIOME-BGC also reproduces more accurately
 351 the dynamics of SWC. The E index is approximately 0.5 in the case of
 352 transpiration (0.532 in the calibration and 0.544 in the validation) while the same
 353 index in the case of SWC is higher than 0.7 (0.766 in the calibration and 0.715 in
 354 the validation). In any case, the obtained results were satisfactory in both,
 355 transpiration and SWC.

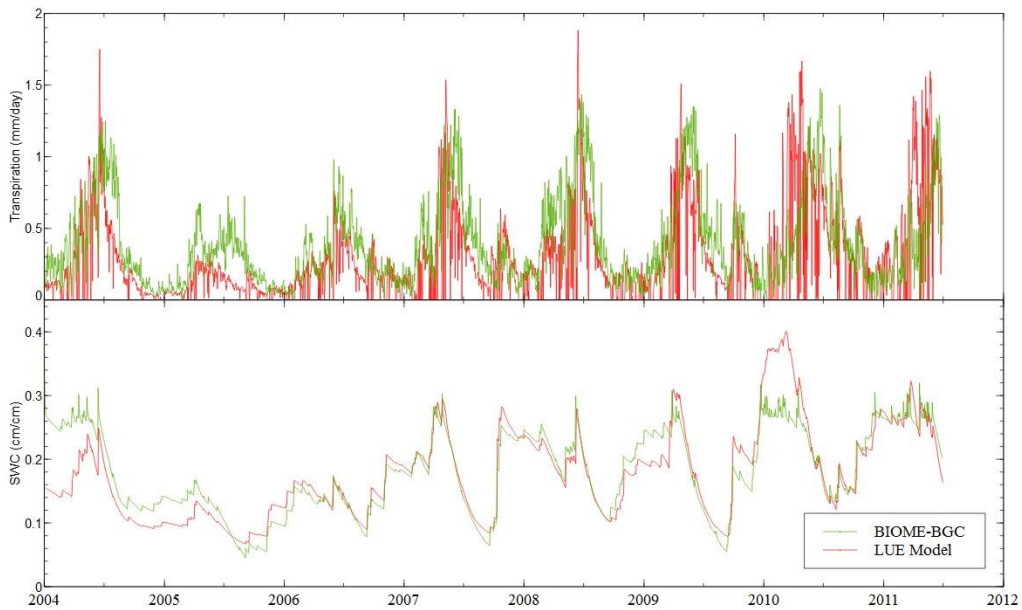
356 Therefore, both models reproduce with acceptable accuracy the water dynamics
 357 of the study site. In fact, the E indexes in terms of SWC is higher than 0.65 for

358 both models (Table II). However, as it was expected and it is shown by the
 359 selected goodness of fit indexes, the BIOME-BGC appears to be more accurate
 360 than the LUE-Model (see Figure 4 and Table II).

361 Table II. Results of the validation using field data for the LUE and Biome-BGC
 362 models (observational period 27/03/2008 to 31/05/2011)

	Transpiration		SWC	
	LUE-Model	Biome-BGC	LUE-Model	Biome-BGC
E	0.346	0.544	0.65	0.715
RMSE	0.274	0.209	0.051	0.070

363 Comparing the results of both models in a longer run (from 2004 to 2012
 364 approximately), we can observe that there are not big differences between them
 365 (see Figure 5). The agreement between SWC time series is very strong and it is
 366 better than the agreement between transpiration time series. But, in general,
 367 there are not big differences. In fact, the Pearson correlation coefficient values
 368 between them are 0.638 and 0.865 for the transpiration and SWC respectively.



369

370 Figure 5. Transpiration and SWC time series simulated by both models (from 2004 to 2012
 371 approximately)

372 Likewise, when estimating the general B/G rate during the dry and the wet years,
 373 the models produce very similar results, with a rate around 0.1 during the dry
 374 year and around 0.8 during the wet year (Table III).

375 Table III. Results of each model in terms of blue (excedence) and green (evapotranspiration) water

	Flows	Dry year (2005)	Wet year (2010)
LUE-Model	Precipitation (mm)	188	739
	Evapotranspiration (mm)	165.18	431.87
	Excedence (mm)	16.34	326.93
	B/G	0.098	0.757
Biome-BGC	Precipitation (mm)	188	739
	Evapotranspiration (mm)	156.30	408.80
	Excedence (mm)	31.7	330.10
	B/G	0.104	0.807

376 8. Discussion

377 In general, LUE and BIOME-BGC reproduced with acceptable accuracy SWC
378 and transpiration values. Both models simulated more accurately SWC than
379 transpiration dynamics, and a disagreement between simulated and observed
380 daily transpiration can be found at certain periods for both models. The
381 disagreement could be due to the fact that 2010 was an abnormally rainy period,
382 and as an outlier, the models might not reproduce it properly. However, since the
383 periods where the models performed with less accuracy were not the same, the
384 high quantity of rain might not be the cause, or at least not the main one. Del
385 Campo *et al* 2014 grouped the simulated period in four spells according to the
386 precipitation and the average daily temperature: Dry Cool (DC), Dry Warm (DW),
387 Wet Cool (WC) and Wet Warm (WW). Analyzing the performance of both models
388 during each spell, it is possible to observe that both models behave different. The
389 LUE model does not reproduce accurately cool spells, either dry or wet, while the
390 BIOME-BGC is slightly less accurate when simulating dry spells, either cool or
391 warm. Analyzing the field data, it is possible to observe a significant linear
392 relationship between transpiration and Vapor Pressure Deficit (VPD) during cool
393 spells, which is stronger during WC spells. Contrarily, during warm spells, the
394 transpiration is significantly correlated to the measured SWC. This behavior
395 describes the general dynamics of the vegetation, where if soil water availability
396 does not limit transpiration, it is expected that transpiration will be affected
397 primarily by atmospheric evaporative demands (Monteith, 1965; Tanner and
398 Fuchs, 1968). Thus, the LUE model appears not to include properly the
399 atmospheric evaporative demands, and its performance during the periods were
400 this demand prevails over SWC is less accurate.

401 With regards to the lower performance of the BIOME-BGC model when
402 simulating transpiration during dry spells, is probably due to the fact that the
403 model is not originally designed to reproduce arid or semi-arid environments.
404 Indeed the fact that SWC is always accurately simulated indicates that the
405 drought tolerance of semi-arid species might reduce the accuracy of the model at
406 certain periods.

407 As mentioned previously, when analyzing the performance of the LUE model with
408 satellite information, we observed that the main disagreement between LAI_r and
409 NDVI is produced during the period from July 2004 to December 2005, which
410 was an extremely dry period. The precipitation during this period was 188 mm,
411 which is significantly lower than the annual mean precipitation registered in the
412 study site (466 mm). Thus, according to the general dynamics of the vegetation,
413 in this extremely dry period the SWC would be expected to be the main driving
414 factor of transpiration, and therefore, the performance of the LUE model is
415 expected to be more accurate. SWC and LAI_r are highly correlated in the LUE
416 model, and a significantly decrease in SWC will also imply a significantly
417 decreasing of LAI_r. However, the immediate response of LAI_r to SWC variations
418 contrasts to that of NDVI, which appears to be delayed a few months. NDVI
419 values of arid or semiarid areas, as well as those of Mediterranean areas during
420 the dry summer season, have been demonstrated to be strongly dependent on
421 plant water availability in preceding months (Maselli 2004). In particular, inter-
422 year NDVI variations of Mediterranean vegetation cover are mostly controlled by
423 variations in previous plant water stress conditions during the arid season (Caroti
424 *et al.*, 1995 and Cannizzaro *et al.*, 2002). Maselli 2004 found a strong
425 dependence of a Mediterranean pine wood summer NDVI values on winter

426 rainfalls and summer NDVI were causally linked; i.e., the first was the main cause
427 for the latter. Besides, as a drought-avoiding species, *Pinus halepensis* has an
428 ability to survive intense and prolonged drought (Maseyk *et al.*, 2008; Schiller and
429 Atzmon 2009) that could delay even more the NDVI response. Thus, the
430 disagreement between LAI_r and NDVI found in this study is probably due to the
431 late response of NDVI to a severe drought period. Indeed, after this drought
432 period, NDVI decreases until August 2006, where the regression between LAI_r
433 and NDVI, although significant (sig. < 0.05) showed a low regression coefficient
434 of 0.2. Contrarily, from August 2006 onwards, NDVI starts to increase again
435 probably as a response of the rain during the winter of 2006, and the regression
436 coefficient increases to 0.69.

437 Likewise, the disagreement between LAI_r and NDVI during the first half of 2010
438 can also be due to the late response of NDVI to changes in water availability,
439 although in this case the water availability increases substantially as 2010 was an
440 abnormally rainy period. As a consequence, LAI_r increases and remains with
441 high values almost the first half of 2010. On the contrary, the increasing of NDVI
442 is not observed until August, when the regression coefficient between LAI_r and
443 NDVI increases from 0.29 to 0.61. However, with these exceptions, the LUE
444 model captures well the dynamic of the vegetation provided by NDVI.

445 Likewise, the estimation of the general B/G water balance using the LUE and the
446 BIOME-BGC model produced very similar results when simulating both dry and
447 wet years. Both models obtained a B/G water ratio below 1, where more than half
448 of the total annual rainfall would be consumed by the ecosystem and returned to
449 the atmosphere, and a short quantity of water would be able to supply the

450 catchment. The similarity of the results enhances the capability of the
451 parsimonious LUE-Model to distribute water, which is very similar to that of the
452 physically-based Biome-BGC model. A proper distribution of blue and green
453 water is essential for a model as it raises the question of a loss of services that
454 ecosystems provide to human and also the amount of available water to be used
455 by vegetation. Particularly, in Mediterranean ecosystems, where the global
456 climate change scenario predicts an increase in dry years over normal and wet
457 periods (Giorgi and Lionello, 2008), an accurate distribution of the blue and green
458 water is fundamental when designing water management policies.

459 **9. Conclusions**

460 The obtained results in this research suggest that the parsimonious model is able
461 to adequately reproduce the dynamics of vegetation (the correlation coefficient
462 with the satellite and field transpiration data are acceptable), and it also
463 reproduces properly the soil moisture variations. In other words, it has been
464 shown that a parsimonious model with simple equations can achieve good
465 results in general terms, and it is possible to assimilate satellite information for
466 the model implementation. However, it also has been observed that the LUE
467 model's accuracy is worse when the transpiration is limited by the atmospheric
468 demands. It's important to mention that the LUE model uses the reference
469 evapotranspiration during the calculation of the transpiration. As the LUE model
470 implementation represented such situation in which there are not field
471 information, the reference evapotranspiration was calculated by Hargreaves and
472 Samani method (this method only needs information of temperatures and

473 radiation). Maybe the LUE model's performance can improve if the Penman
474 Monteith method was used to calculate the reference evapotranspiration.

475 Anyway, the objective of this paper is not to propose a 'perfect model'. In fact, we
476 want to know if a simple model implemented only using satellite data can be used
477 as alternative against a well-known physically-based model implemented using
478 field measurements. The comparison between both models in a long period
479 shows there are not big differences between them, and the dynamics in both
480 cases (transpiration and SWC) are very similar.

481 In this research, the satellite data played a key role in the implementation of the
482 model. In fact, the measured transpiration data were available only over less than
483 two years as a field observation of the vegetation state and evolution. In this
484 case, the satellite data was a very useful source of information, and its
485 combination with the parsimonious LUE model has demonstrated to be an
486 accurate tool capable of predict the role of the vegetation in the water cycle with
487 no field data.

488 **ACKNOWLEDGEMENTS**

489 The research leading to these results has received funding from the Spanish
490 Ministry of Economy and Competitiveness through the research projects
491 INTEGRA (ref. CGL2011-28776-C02) and E-HIDROMED (ref. CGL2014-58127-
492 C3). The MODIS data were obtained through the online Data Pool at the NASA
493 Land Processes Distributed Active Archive Center (LP DAAC), USGS/Earth
494 Resources Observation and Science (EROS) Center, Sioux Falls, South Dakota

495 (https://lpdaac.usgs.gov/get_data). The meteorological data were provided by the
496 Spanish National Weather Agency (AEMET).

497 REFERENCES

498 Allen, R.G., Pereira, L.S., Raes, D., Smith, M. & others. *Crop*
499 *evapotranspiration-Guidelines for computing crop water requirements-FAO*
500 *Irrigation and drainage paper 56*. FAO, Rome, 1998, 300, 6541.

501 Alvenäs, G.; Jansson, P. Model for evaporation, moisture and temperature of
502 bare-soil: calibration and sensitivity analysis. *Agr. Forest Meteorol.*, 1997, 88,
503 47-56

504 Andersen, F.H. *Hydrological modeling in a semi-arid area using remote*
505 *sensing data*. Doctoral Thesis, Department of Geography and Geology,
506 University of Copenhagen (Denmark), 2008.

507 Aydin, M.; Ynag, S.L.; Kurt, N.; Yano, T. Test of a simple model for
508 estimating evaporation from bare-soils in different environments. *Ecol. Model.*,
509 2005, 182, 91-105

510 Blösch G., Sivapalan M. Scales issues in hydrological modelling. A review.
511 In: Kalma J.D., Sivapalan M. (Eds). *Scales issues in Hydrological Modelling*. John
512 Wiley & sons. Ltd. Chichester, uk. (chapter 2), 1996, 9-48.

513 Burgess, S.S.SO.; Adams, M.A.; Turner, N.C.; Beverly, C.R.; Ong, C.K.;
514 Jhan, A.A.H; Bleby, T.M. An improved heat pulse method to measure low and
515 reverse rates of sap flow in woody plants. *Tree Physiology*, 2001, 21, 589-598.

516 Calatayud, V., Muñoz, C., Hernández, R., Sanz, M.J., Pérez Fortea, V.,
517 Soldevilla, C., Sánchez, G. Seguimiento de daños en acículas de *Pinus*
518 *halepensis* en localidades de Teruel y Castellón (España). *Ecología*, 2000, 14,
519 129–140.

520 Cannizzaro, G., Maselli, F., Caroti, L., Bottai, L. Use of NOAA-AVHRR NDVI
521 data for climatic characterization of Mediterranean areas N.A. Geeson, G.J.
522 Brandt, J.B. Thornes (Eds.), *Mediterranean desertification: A mosaic of*
523 *processes and responses*, Wiley, The Atrium, Southern Gate, Chichester, West
524 Sussex PO19 8SQ, UK, 2002, 47–54.

525 Caroti, L., Maselli, F., Serafini, C. Valutazione dell'informazione
526 agrometeorologica contenuta in profili NOAA-NDVI Proceedings of VII AIT
527 National Congress, Chieri (Torino, Italy), 17–20 October, 1995, 487–492

528 Ceballos, Y. & Ruiz de la Torre, J. *Árboles y arbustos de la España*
529 *peninsular*, ETSI Montes Publications, Madrid, 1979.

530 Chiese, M.; Maselli, F.; Moriondo, M.; Fibbi, L.; Bindi, M.; Running, S.
531 Application of Biome-BGC to simulate Mediterranean forest processes.
532 *Ecological Modelling*, 206, 2007, 179-190.

533 Dawson, T.P.; Curran, P.J.; Plummer, S.E. LIBERTY-modeling the effect of
534 leaf biochemical contraction on reflectance spectra. *Remote Sens. Environ.*,
535 1998, 65, 50-60

536 Del Campo, A.D.; Fernandes, T.J.G.; Molina, A.J. Hydrology-oriented
537 (adaptive) silviculture in a semiarid pine plantation: How much can be modified

538 the water cycle through forest management?. *European Journal of Forest*
539 *Research*, 2014, 133, 879-894.

540 Field, C.B.; Randerson, J.T.; Malmstrom, C.M. Global net primary production:
541 combining ecology and remote sensing. *Remote Sens. Environ.*, 1995, 51, 74-88

542 Francés, F., Velez, J.I. & Vélez, J.J. Split-parameter structure for the
543 automatic calibration of distributed hydrological models. *Journal of Hydrology*,
544 2007, 332, 226–240.

545 Gamon, J.A.; Serrano, L.; Surfus, J.S. The photochemical reflectance index:
546 an optical indicator of photosynthetic radiation use efficiency across species,
547 functional types, and nutrient levels. *Oecologia*, 1997, 112, 492-501

548 Gerten, D.; Schaphoff, S.; Haberlandt, U.; Lucht, W.; Sitch, S. Terrestrial
549 vegetation and water balance – hydrological evaluation of a dynamic global
550 vegetation model. *Journal of Hydrology*, 2004, 286 (1-4), 249-270.

551 Giorgi, F.; Lionello, P. Climate change projections for the Mediterranean
552 region. *Global Planet Change*, 63 (2-3), 2008, 90-104

553 González-Sanchis, M.; del Campo, A.D.; Molina, A.J.; Fernandes, T.J.G..
554 Modelling adaptive forest management of a semi-arid Mediterranean Aleppo pine
555 plantation. *Ecological Modelling*, 2015, in press.

556 Guswa, A.J.; Celia, M.A.; Rodriguez-Iturbe, I. Effect of vertical resolution on
557 predictions of transpiration in water-limited ecosystems, *Adv. Water Resour.*,
558 2004, 27, 467-480

559 Hernandez-Santana, V.; Asbjornsen, H.; Sauer, T.; Isenhardt, T.; Schilling, K.;
560 Schultz, R. Enhanced transpiration by riparian buffer trees in response to
561 advection in a humid temperature agricultural landscape. *For. Ecol. Manag.*,
562 2011, 261, 1415-1427.

563 Huxman, T.E.; Wilcox, B.P.; Breshears, D.D.; Scott, R.L.; Snyder K.A.; Small,
564 E.E.; Hultine, K.; Pockman, W.T.; Jackson, R.B. Ecohydrological implication of
565 woody plant encroachment, *Ecological Society of America*, 2005, 86(2), 308-319.

566 Jackson, R.D.; Huete, A.R. Interpreting vegetation indices. *Preventive*
567 *Veterinary Medicine*, 1991, 11, 185–200.

568 Laio, F.; Porporato, A.; Ridolfi, L.; Rodriguez-Iturbe, I. Plants in water-
569 controlled ecosystems: active role in hydrologic processes and response to water
570 stress. II. Probabilistic soil moisture dynamics. *Adv. Water Resour*, 2001, 24,
571 707–723.

572 Landsber, J.J; Waring, R.H. A generalised model of forest productivity using
573 simplified concepts of radiation-use efficiency, carbon balance and partitioning.
574 *Forest Ecol. Manag.*, 1997, 95, 209-228

575 Lee, T.J., Pielke, R.A. Estimating the soil surface specific humidity, *J. Appl.*
576 *Meteorol.*, 1992, 31, 480-484.

577 Maselli, F.; Chiesi, M.; Moriondo, M.; Fibbi, L.; Bindi, M.; Running, S.
578 Modelling the forest carbon budget of a Mediterranean region through the
579 integration of ground and satellite data. *Ecological Modelling*, 220, 2009, 330-
580 342.

581 Maselli, F. Monitoring forest conditions in a protected Mediterranean coastal
582 area by the analysis of multiyear NDVI data, *Remote Sensing of Environment*,
583 2004, 89, 4, 423-433.

584 Masey. k K, Lin T, Rotenberg E, Grünzweig JM, Schwartz A, Yakir D.
585 Physiology-phenology interactions in a productive semi-arid pine forest. *New*
586 *Phytologist*, 2008, 178, 603–16.

587 McCree, K.J. The action spectrum, absorptance and quantum yield of
588 photosynthesis in crop plants. *Agricultural Meteorology*, 1972, 9, 191–216.

589 Molina, A.; Del Campo, A.D. Leaf area index estimation in a pine plantation
590 with LAI-2000 under direct sunlight conditions: relationship with inventory and
591 hydrological variables. *Forest Systems*, 20 (1), 2012, 108-121.

592 Molina, A.; del Campo, A.D. The effects of experimental thinning on
593 throughfall and stemflow: A contribution towards hydrology-oriented silviculture in
594 Aleppo pine plantations. *Forest Ecol. Manag*, 2012, 269, 206–213

595 Montaldo, N.; Rondena, R.; Albertson, J.D.; Mancini, M. Parsimonious
596 modeling of vegetation dynamics for ecohydrologic studies of water-limited
597 ecosystems. *Water Resour. Res.*, 2005, 41, W10416

598 Monteith, J.L. Evaporation and environment. In: *The State and Movement of*
599 *Water in Living Organisms*. Proc. 19th Syrup. Soc. Exp. Biol., Swansea.
600 Academic Press, New York, 1965, 205-234.

601 Mu, Q., Zhao, M. & Running, S.W. Improvements to a MODIS global
602 terrestrial evapotranspiration algorithm. *Remote Sensing of Environment*, 2011,
603 115, 1781–1800.

604 Ollinger, S.V.; Richardson, A.D.; Martin, M.E.; Hollinger, D.Y.; Frohking, S.;
605 Reich, P.B.; Plourde, L.C.; Katul, G.; Munger, J.W.; Oren, R.; Smith, M.L.; Paw,
606 U.; Bolstad, K.T.; Cook, P.V.; Day, B.; Martin, M.C.; Monson, T.A.; Schmidt,
607 R.K.H.P. Canopy nitrogen, carbon assimilation, and albedo in temperate and
608 boreal forests: functional relations and potential climate feedbacks. *Proc. Natl.*
609 *Acad. Sci. USA*. 2008, 105, 19335-19340

610 Parlange, M.B.; Katul, G.G. Estimation of the diurnal variation of potential
611 evaporation from a wet bare-soil surface, *J. Hydrol.*, 1992, 132, 71-89.

612 Pasquato M. *Comparison of parsimonious dynamic vegetation modeling*
613 *approaches for semiarid climates*. PhD Thesis, Universitat Politècnica de
614 València, 2013.

615 Pasquato, M.; Medici, M.; Friend A.D.; Francés, F. Comparing two
616 approaches for parsimonious vegetation modelling in semiarid regions using
617 satellite data. *Ecohydrology*, 2014, DOI: 10.1002/eco.1559

618 Pietsch, S.; Hasenauer, H.; Kucera, J.; Cermak, J. Modelling effects of
619 hydrological changes on the carbon and nitrogen balance of oak in floodplains.
620 *Tree physiology*, 23 (11), 2003, 735-746

621 Pilgrim, D.H.; Chapman, T.G.; Doran, D.G. Problems of rainfall-runoff
622 modelling in arid and semiarid regions, *Hydrological Sciences Journal - des*
623 *Sciences Hydrologiques*, 1988, 33, 379-400.

624 Quevedo, D.I.; Francés, F. A conceptual dynamic vegetation-soil model for
625 arid and semiarid zones. *Hydrology and Earth System Science*, 2008, 12, 1175–
626 1187

627 Rodriguez-Iturbe, I.; Porporato, A.; Laio, F; Ridolfi, L. Plants in water-
628 controlled ecosystems: active role in hydrologic processes and response to water
629 stress. I. Scope and general outline. *Adv. Water Resour.*, 2001, 24, 695–705

630 Running, S.W.; Nemani, R.R.; Heinsch, F.A.; Zhao, M.; Reeves, M.;
631 Hashimoto, H. A continuous satellite-derived measure of global terrestrial primary
632 production. *BioScience*, 2004, 54, 547-560.

633 Sabaté, S.; Gracia, C.A.; Sánchez, A. Likely effects of climate change on
634 growth of *Quercus ilex*, *Pinus halepensis*, *Pinus pinaster*, *Pinus sylvestris* and
635 *Fagus sylvatica* forests in the Mediterranean region. *Forest Ecol. Manag.*, 2002,
636 162, 23-37.

637 Schiller G, and Atzmon N. 2009. Performance of Aleppo pine (*Pinus*
638 *halepensis*) provenances grown at the edge of the Negev desert: a review.
639 *Journal of Arid Environments* 73: 1051–7.

640 Schimel, D.A.; Braswell, B.H.; Holland, E.A.; McKeown, R.; Ojuna, D.S.;
641 Painter, T.H.; Parton, W.J.; Townsend, A.R. Climatic, edaphic, and biotic controls

642 over storage and turnover of carbon in soils. *Global Geophysical cycles*, 8 (3),
643 1994, 279-293.

644 Sims, D.A.; Luo, H.; Hastings, S.; Oechel, W.C.; Rahman, A.F.; Gamon, J.A.
645 Parallel adjustments in vegetation greenness and ecosystem CO₂ exchange in
646 response to drought in a Southern California chaparral ecosystem. *Remote Sens.*
647 *Environ.*, 2006, 103, 289-303

648 Snyder, R.L.; Bali, K.; Ventura, F.; Gómez-MacPherson, H. Estimating
649 evaporation from bare and nearly bare soil, *J. Irrig. Drain. E.-ASCE*, 2000, 126,
650 399-403.

651 Sprintsin, M.; Karnieli, A.; Berliner, P.; Rotenberg, E.; Yakir, D.; Cohen, S.
652 The effect of spatial resolution on the accuracy of leaf area index estimation for a
653 forest planted in the desert transition zone. *Remote Sens. Environ.*, 2007, 109,
654 416-428

655 Tanner, C.B. and Fuchs, M., Evaporation from unsaturated surfaces: a
656 generalized combination method. *J. Geophys. Res.*, 1968, 73: 1299-1304.

657 Tatarinov, F.; Cienciala E. Application of BIOME-BGC model to managed
658 forests. 1. Sensitivity analysis. *Forest, ecology and management*, 237, 2006,
659 267-279.

660 Thorton, P.; Law, B.; Gholz, H.L.; Clark, K.L.; Falge, E.; Ellsworth, D.;
661 Goldstein, A.; Monson, R.; Hollinger, D.; Falk, M.; Chen, J.; Sparks, J. Modeling
662 and measuring the effects of disturbance history and climate on carbon and

663 water budgets in evergreen needleleaf forests. *Agricultural and Forest*
664 *Meteorology*, 2002, 113, 185-222

665 Vicente-Serrano, S.M.; Lasanta, T.; Gracia, C. Aridification determines
666 changes in forest growth in *Pinus halepensis* forests under semiarid
667 Mediterranean climate conditions. *Agricultural and Forest Meteorology*, 2010,
668 150, 614–628.

669 Walker, B.H.; Langridge, J.L. Modelling plant and soil water dynamics in
670 semiarid ecosystems with limited site data, *Ecol. Model.*, 1996, 87, 153-167.

671 Williams, C.A.; Albertson, J.D. Contrasting short and long-timescale effects of
672 vegetation dynamics on water and carbon fluxes in water-limited ecosystems.
673 *Water Resour. Res.*, 2005, 41, W06005

674 Williams, D.G.; Cable, W.; Hultine, K.; Hoedjes, J.C.B; Yopez, E.A.;
675 Simonneaux, V.; Er-Raki, S.; Boulet, G.; Bruin, H.A.R.; Chehbouni A.;
676 Hartogensis, O.K.; Timouk, F. Evapotranspiration components determined by
677 stable isotopes, sap flow and eddy covariance techniques. *Agric. For. Meteorol.*,
678 2004, 125, 241-258.

679 Zhang, Y.Q.; Viney, N.R.; Chiew, F.H.S.; van Dijk, A.I.J.M.; Lin, Y.Y.
680 Improving hydrological and vegetation modeling using regional model calibration
681 schemes together with remote sensing data. *19th International Congress on*
682 *Modelling and Simulation*, Perth, Austria, December 2011.

683